

DP production in e^+ beam dump experiments via resonant e^+e^- annihilation

Cristian David Ruiz Carvajal

Phys. Rev. D 97, 095004 (2018)

E. Nardi, A. Ghoshal, D. Meloni, M. Raggi

26/11/2018



Outline

Hidden Sector

→ Dark photons

Beam dump experiments

→ Production modes for DP searches

Proposal

→ Production via resonant annihilation

** Peculiarities and advantages

A specific goal

→ Testing the ^8Be anomaly for the 17 MeV DP

Results and conclusions

Hidden Sector

A new sector containing new particles as well as new interactions. **New physics beyond the SM**



A rich structure itself, with DM making up only a part of it.
→ New **light weakly-coupled particles**, well below the Weak-scale that interact only feebly with ordinary matter.

Hidden Sector

A new sector containing new particles as well as new interactions. **New physics beyond the SM**



A rich structure itself, with DM making up only a part of it.
→ New **light weakly-coupled particles**, well below the Weak-scale that interact only feebly with ordinary matter.

The HS is motivated by theoretical considerations in many extensions to the SM, where the new particles appear naturally when symmetries are broken at high energy scales.

U(1) Global

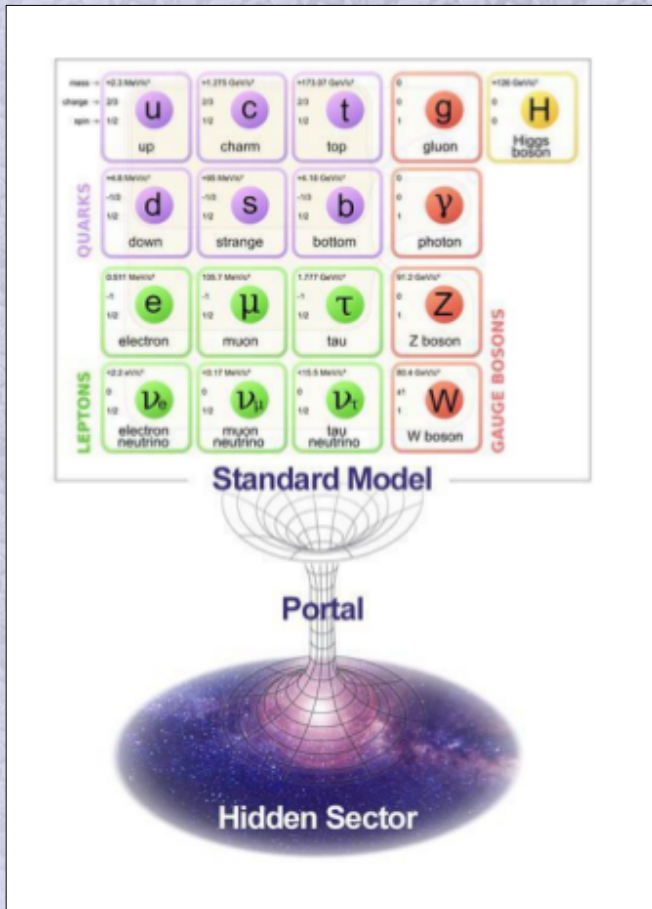
U(1) Gauge

Hidden Sector

Besides gravity, there are only a few well-motivated interactions allowed by SM symmetries that provide a “**portal**” from the SM sector into the dark sector.

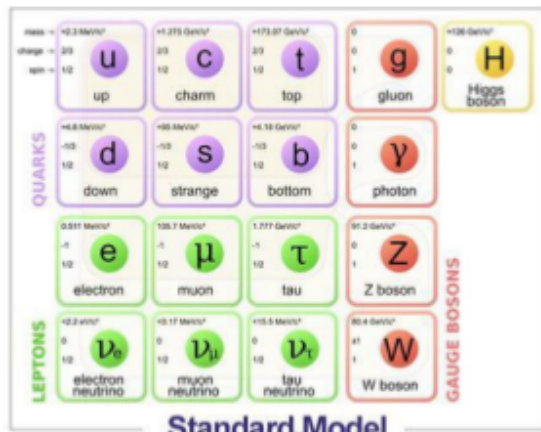
Hidden Sector

Besides gravity, there are only a few well-motivated interactions allowed by SM symmetries that provide a **“portal”** from the SM sector into the dark sector.



Hidden Sector

Besides gravity, there are only a few well-motivated interactions allowed by SM symmetries that provide a **“portal”** from the SM sector into the dark sector.



Standard Model

Portal

Hidden Sector

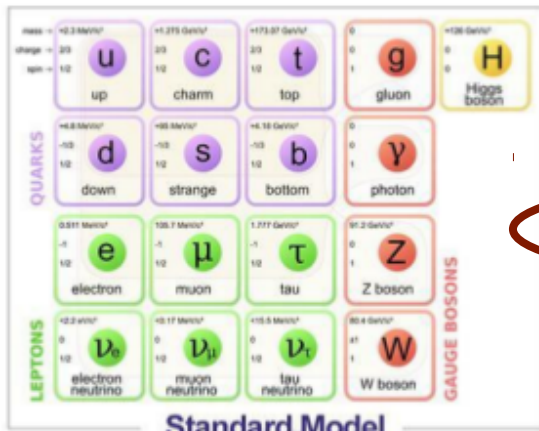
Portal	Particles	Operator
Vector	Dark photon	$-\frac{\epsilon}{2}F'_{\mu\nu}F^{\mu\nu}$
Axion	Pseudoscalars	$\frac{a}{f_a}F_{\mu\nu}\tilde{F}^{\mu\nu}, \frac{a}{f_a}G_{i\mu\nu}\tilde{G}^{i\mu\nu},$ $\frac{\partial_\mu a}{f_a}\bar{\psi}\gamma^\mu\gamma^5\psi$
Higgs	Dark scalars	$(\mu S + \lambda S^2)H^\dagger H$
Neutrino	Sterile neutrino	$y_N\bar{L}HN$

Table 1. Dark sector portals

Andreas et al. arXiv:1311.0029, Jaeckel T. arXiv:1303.1821

Hidden Sector

Besides gravity, there are only a few well-motivated interactions allowed by SM symmetries that provide a **“portal”** from the SM sector into the dark sector.



Standard Model

Portal

Hidden Sector

Portal	Particles	Operator
Vector	Dark photon	$-\frac{\epsilon}{2}F'_{\mu\nu}F^{\mu\nu}$
Axion	Pseudoscalars	$\frac{a}{f_a}F'_{\mu\nu}F^{\mu\nu}, \frac{a}{f_a}G_{i\mu\nu}\tilde{G}^{i\mu\nu},$ $\frac{\partial_\mu a}{f_a}\bar{\psi}\gamma^\mu\gamma^5\psi$
Higgs	Dark scalars	$(\mu S + \lambda S^2)H^\dagger H$
Neutrino	Sterile neutrino	$y_N\bar{L}HN$

Table 1. Dark sector portals

Andreas et al. arXiv:1311.0029, Jaeckel T. arXiv:1303.1821

Dark photons

→ Massive gauge boson arising from a new $U(1)'$ gauge symmetry.

** The mass can arise via the Higgs mechanism (or via the Stückelberg mechanism) and can take on a large range of values in the MeV–GeV range.

Dark photons

→ Massive gauge boson arising from a new $U(1)'$ gauge symmetry. Its dominant interaction with the SM arise solely from: $(\epsilon/2) F'_{\mu\nu} F^{\mu\nu}$

Dark photons

→ Massive gauge boson arising from a new $U(1)'$ gauge symmetry. Its dominant interaction with the SM arise solely from: $(\epsilon/2) F'_{\mu\nu} F^{\mu\nu}$

At low energies (below the EW scale) and for small masses $m_{A'} \ll m_W$.

Effective interaction $\epsilon e A'_\mu J_{EM}^\mu$ suppressed relative to the electron charge.

** Theoretically can be naturally small $\rightarrow 10^{-8} - 10^{-2}$

General case: there is also a mass matrix mixing between the DP and the heavy Z boson of the SM $\rightarrow \epsilon_Z \frac{g}{2 \cos(\theta_W)} J_\mu^{NC} A'^\mu$

Motivations

PHYSICAL REVIEW D **84**, 103501 (2011)

Dark light, dark matter, and the misalignment mechanism

Ann E. Nelson and Jakub Scholtz

(Received 12 July 2011; published 2 November 2011)

Motivations

PHYSICAL REVIEW D **84**, 103501 (2011)

Dark light, dark matter, and the misalignment mechanism

The Muon $(g - 2)$ Theory Value: Present and Future

Thomas Blum¹, Achim Denig², Ivan Logashenko³, Eduardo de Rafael⁴,
B. Lee Roberts⁵, Thomas Teubner⁶, Graziano Venanzoni⁷

Motivations

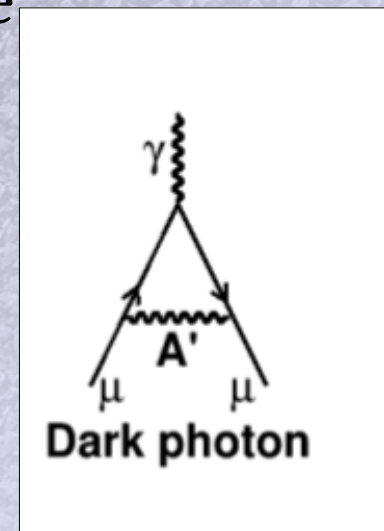
PHYSICAL REVIEW D **84**, 103501 (2011)

Dark light, dark matter, and the misalignment mechanism

The Muon ($g - 2$) Theory Value: Present and Future

Thomas Blum¹, Achim Denig², Ivan Logashenko³, Eduardo de Rafael⁴,
B. Lee Roberts⁵, Thomas Teubner⁶, Graziano Venanzoni⁷

- ** A 3-4 standard-deviation difference with the experimental result.
- ** The ($g - 2$) result is arguably the most compelling indicator of physics beyond the SM.



Motivations

PHYSICAL REVIEW D **84**, 103501 (2011)

Dark light, dark matter, and the misalignment mechanism

The Muon ($g - 2$) Theory Value: Present and Future

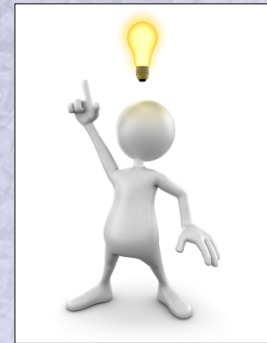
PRL **116**, 042501 (2016)

PHYSICAL REVIEW LETTERS

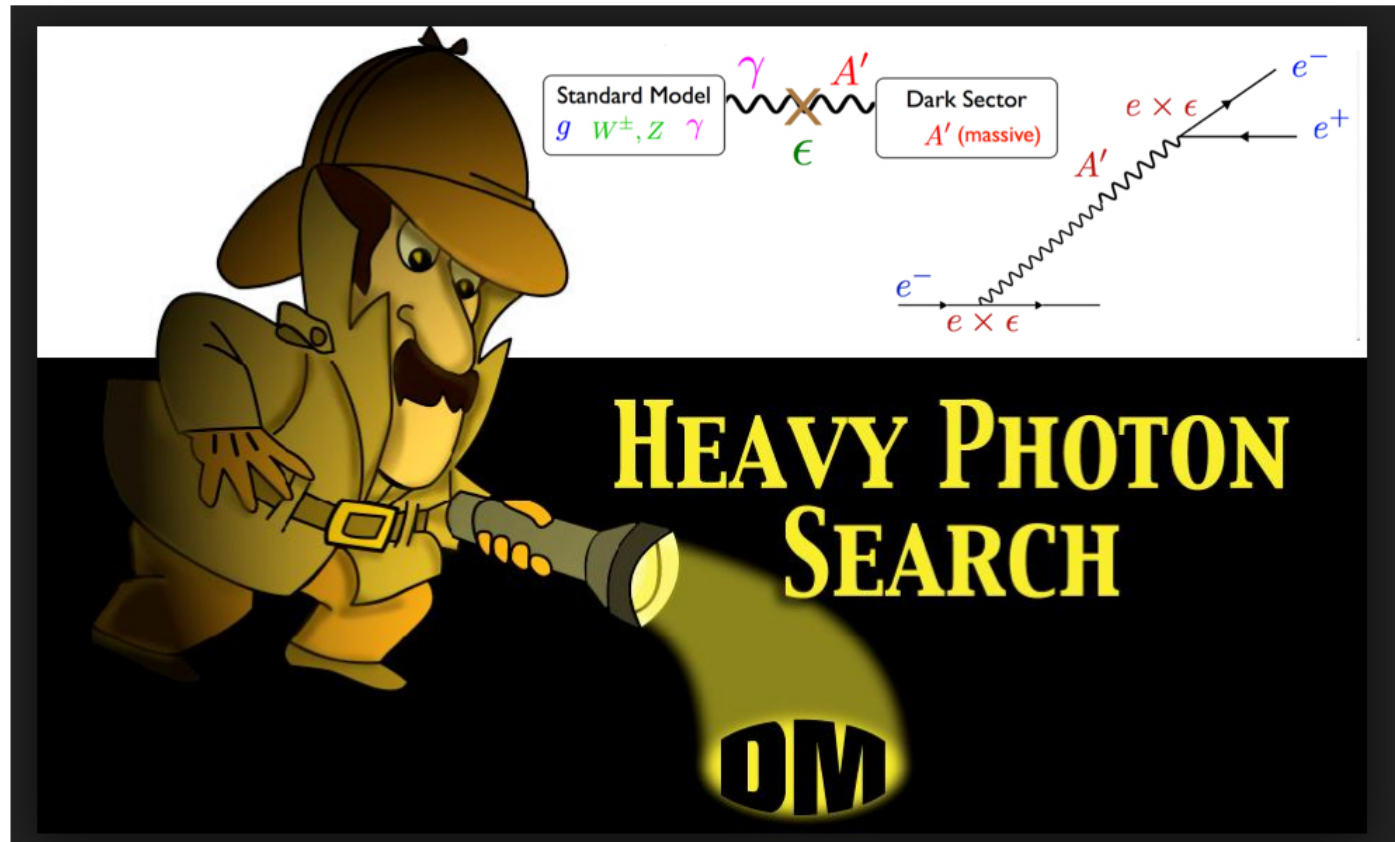
week ending
29 JANUARY 2016

Observation of Anomalous Internal Pair Creation in ^8Be : A Possible Indication of a Light, Neutral Boson

A. J. Krasznahorkay,^{*} M. Csatlós, L. Csige, Z. Gácsi, J. Gulyás, M. Hunyadi, I. Kuti, B. M. Nyakó, L. Stuhl, J. Timár, T. G. Tornyai, and Zs. Vajta



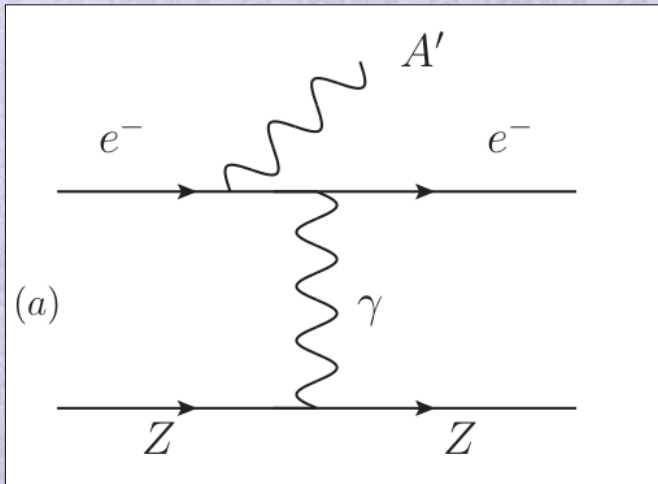
Beam dump experiments



Fixed target experiments for DP searches

1) e^- beams fixed target experiments

→ Electron scattering off nuclei: A' bremsstrahlung

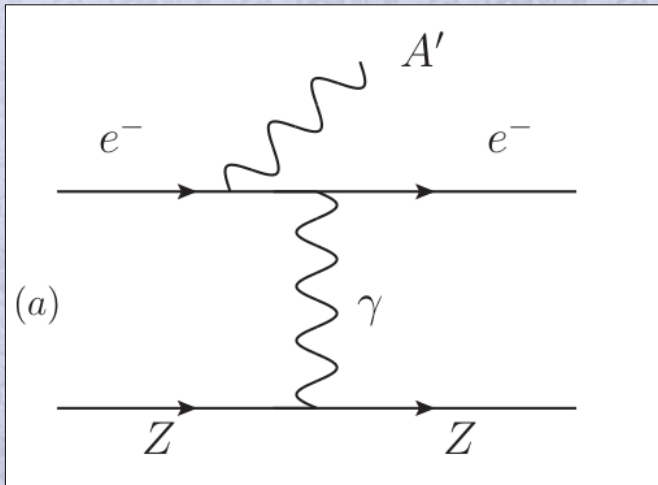


$O(\alpha^3)$ process

Fixed target experiments for DP searches

1) e^- beams fixed target experiments

→ Electron scattering off nuclei: A' bremsstrahlung



$O(\alpha^3)$ process

** Experimental searches

APEX, HPS, DarkLight (JLab) A1,
MAGIX (Mainz), NA64 (CERN),
(SLAC), (Cornell)...

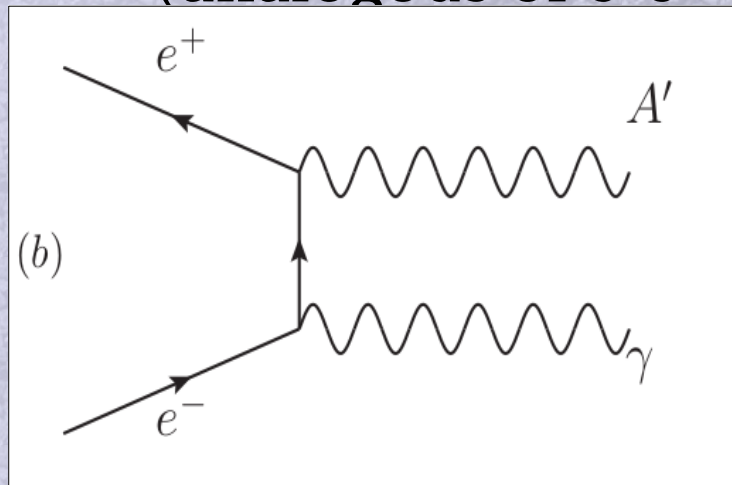
Fixed target experiments for DP searches

1) e^- beams fixed target experiments

→ Electron scattering off nuclei: A' bremsstrahlung

2) e^+ beams fixed target experiments

→ Positron-electron 2-body annihilation
(analogous of $e^+e^- \rightarrow \gamma\gamma$)



$O(\alpha^2)$ process

** Experiments (proposed)

VEPP3 (BINP), PADME (LNF),
MMAAPS (Cornell)

Fixed target experiments for DP searches

1) e^- beams fixed target experiments

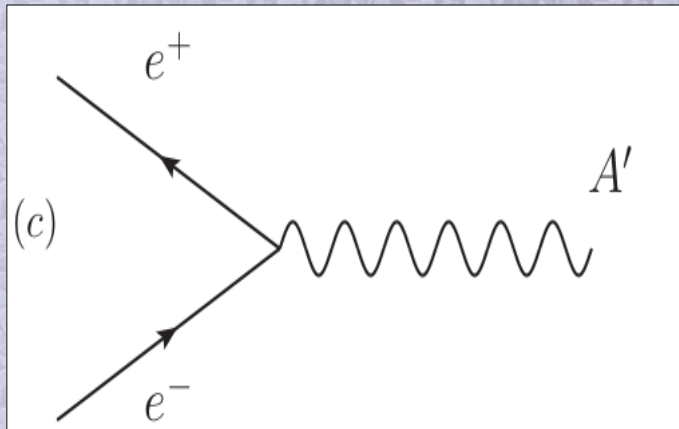
→ Electron scattering off nuclei: A' bremsstrahlung

2) e^+ beams fixed target experiments

→ Positron-electron 2-body annihilation

3) Resonant positron-electron annihilation $e^+e^- \rightarrow A'$

(analogous of $e^+e^- \rightarrow Z$)



Proposal at PADME (LNF)

Fixed target experiments for DP searches

1) e^- beams fixed target experiments

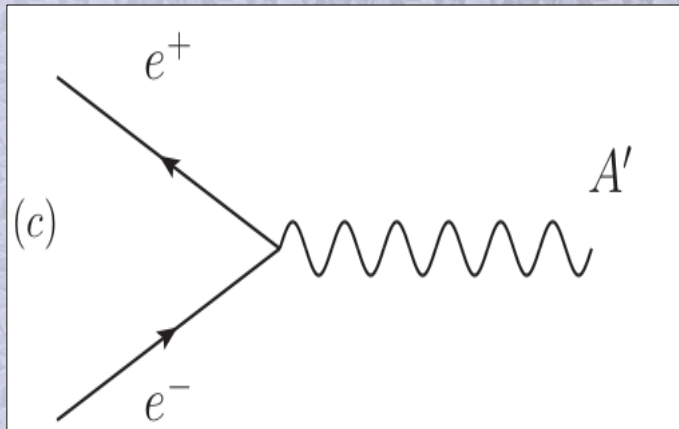
→ Electron scattering off nuclei: A' bremsstrahlung

2) e^+ beams fixed target experiments

→ Positron-electron 2-body annihilation

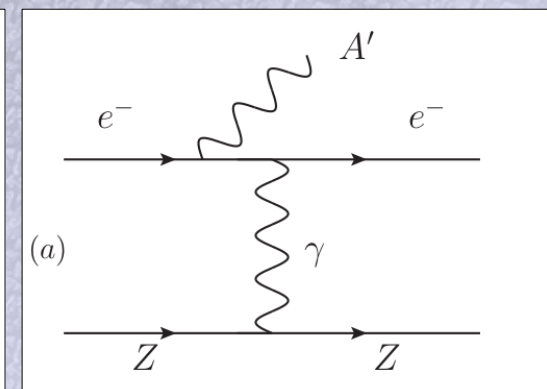
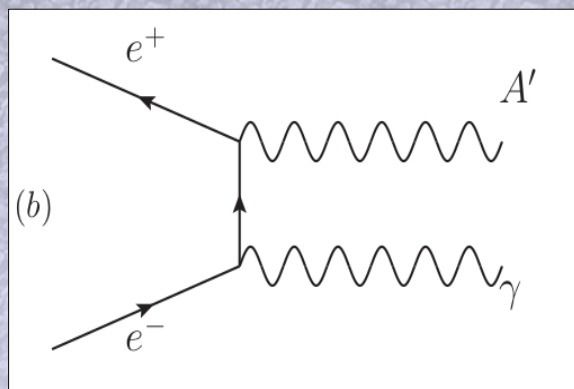
3) Resonant positron-electron annihilation $e^+e^- \rightarrow A'$

(analogous of $e^+e^- \rightarrow Z$)



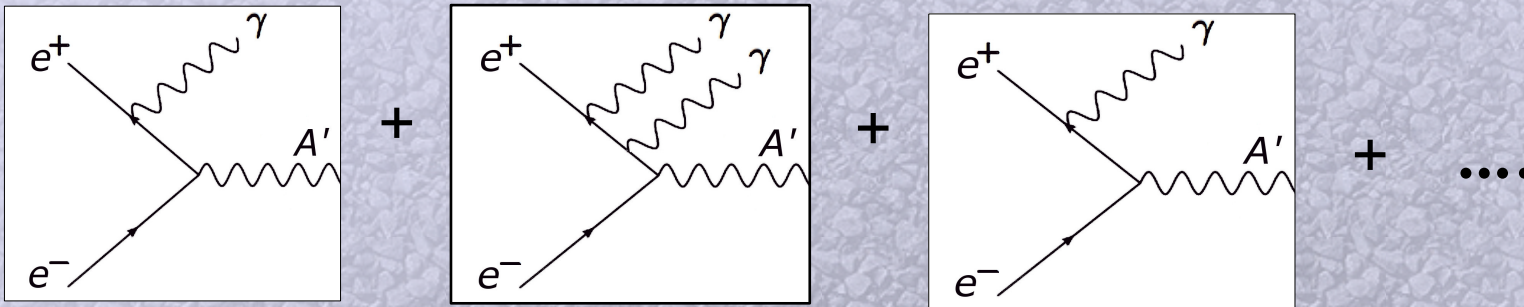
$O(\alpha)$ process

Proposal at PADME (LNF)



Peculiarities and advantages

→ **Radiative return** helps enhancing the cross section by “widening” the resonance.



Up to energies $\Delta E/E \sim 1\%$

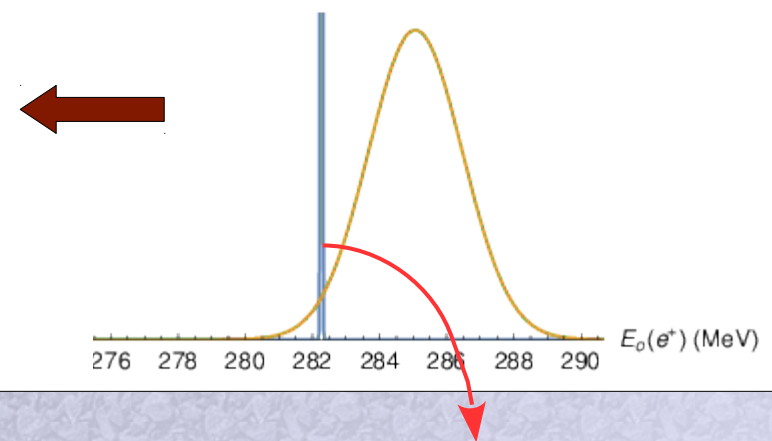
** The emission can radiatively enhance the resonance width, and thus the production rate.

Peculiarities and advantages

- **Radiative return** helps enhancing the cross section by “widening” the resonance.
- Because of the **continuous energy loss** of positrons when propagating through matter, positrons “scan” downward in energy until hitting the resonance.

Peculiarities and advantages

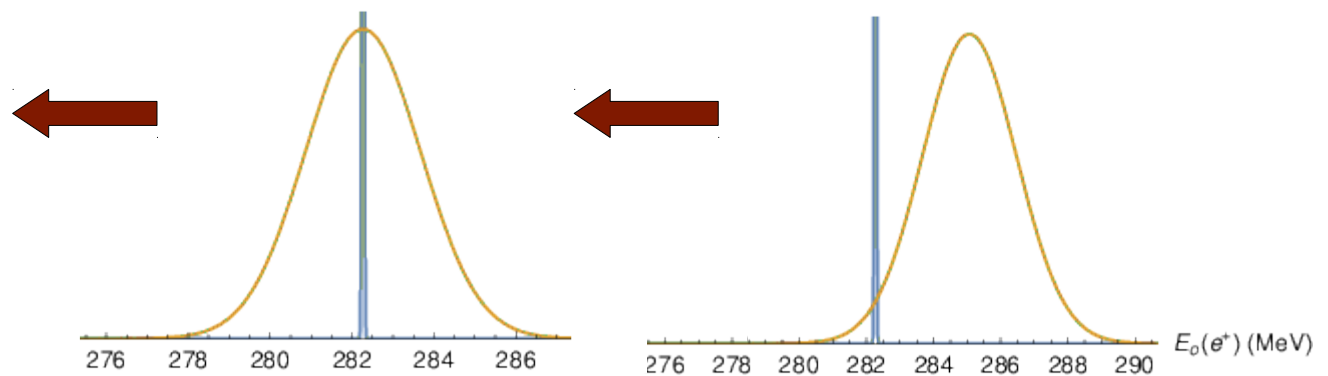
- **Radiative return** helps enhancing the cross section by “widening” the resonance.
- Because of the **continuous energy loss** of positrons when propagating through matter, positrons “scan” downward in energy until hitting the resonance.



$$mA' = 17 \text{ MeV}$$

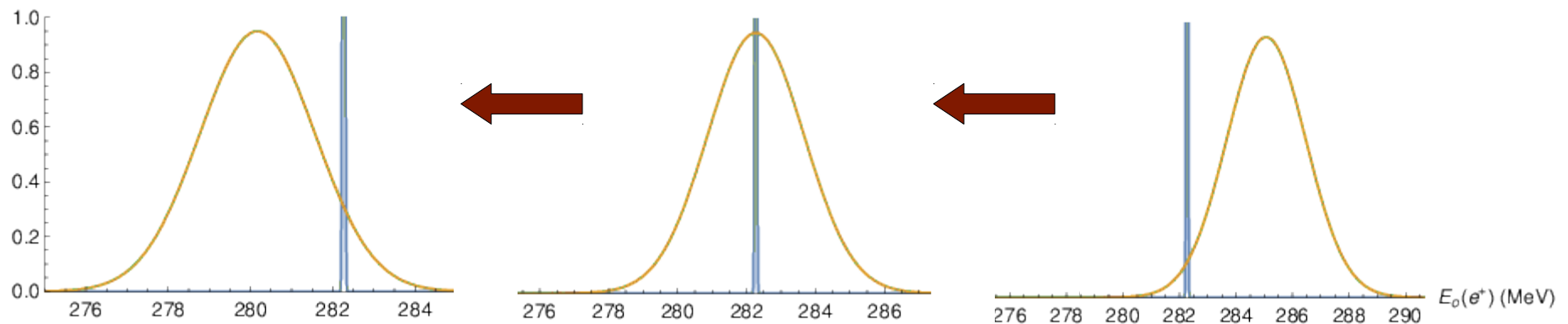
Peculiarities and advantages

- **Radiative return** helps enhancing the cross section by “widening” the resonance.
- Because of the **continuous energy loss** of positrons when propagating through matter, positrons “scan” downward in energy until hitting the resonance.



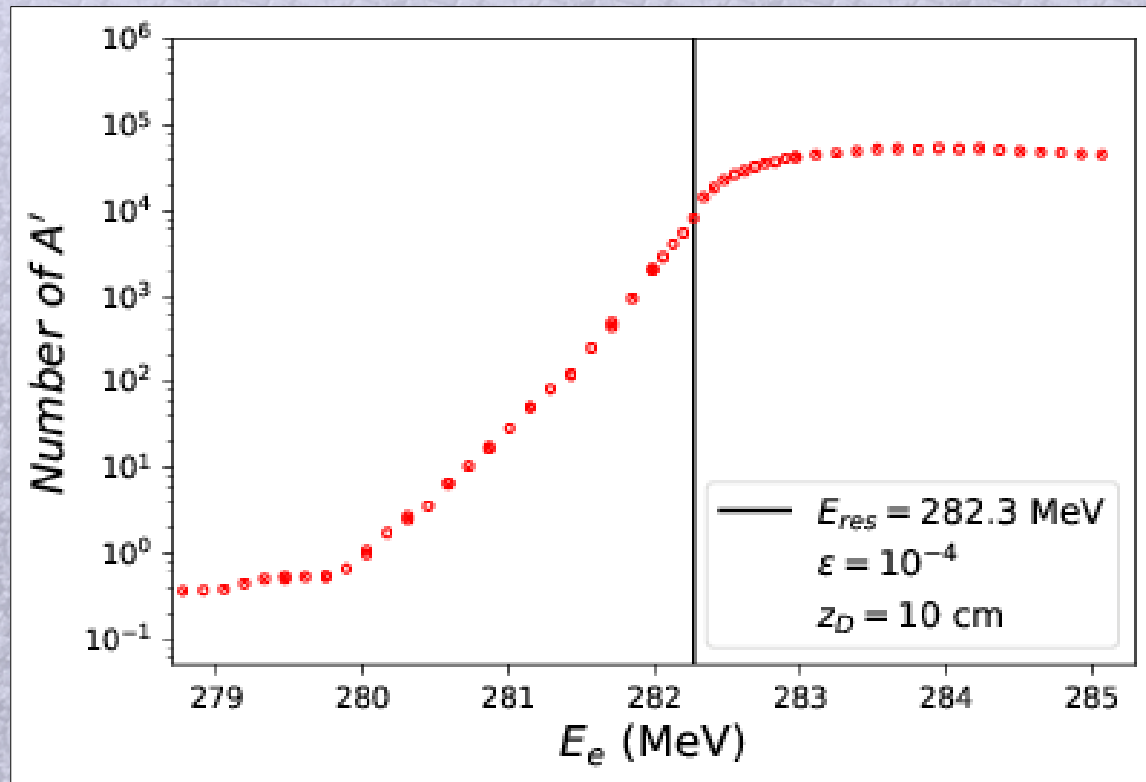
Peculiarities and advantages

- **Radiative return** helps enhancing the cross section by “widening” the resonance.
- Because of the **continuous energy loss** of positrons when propagating through matter, positrons “scan” downward in energy until hitting the resonance.



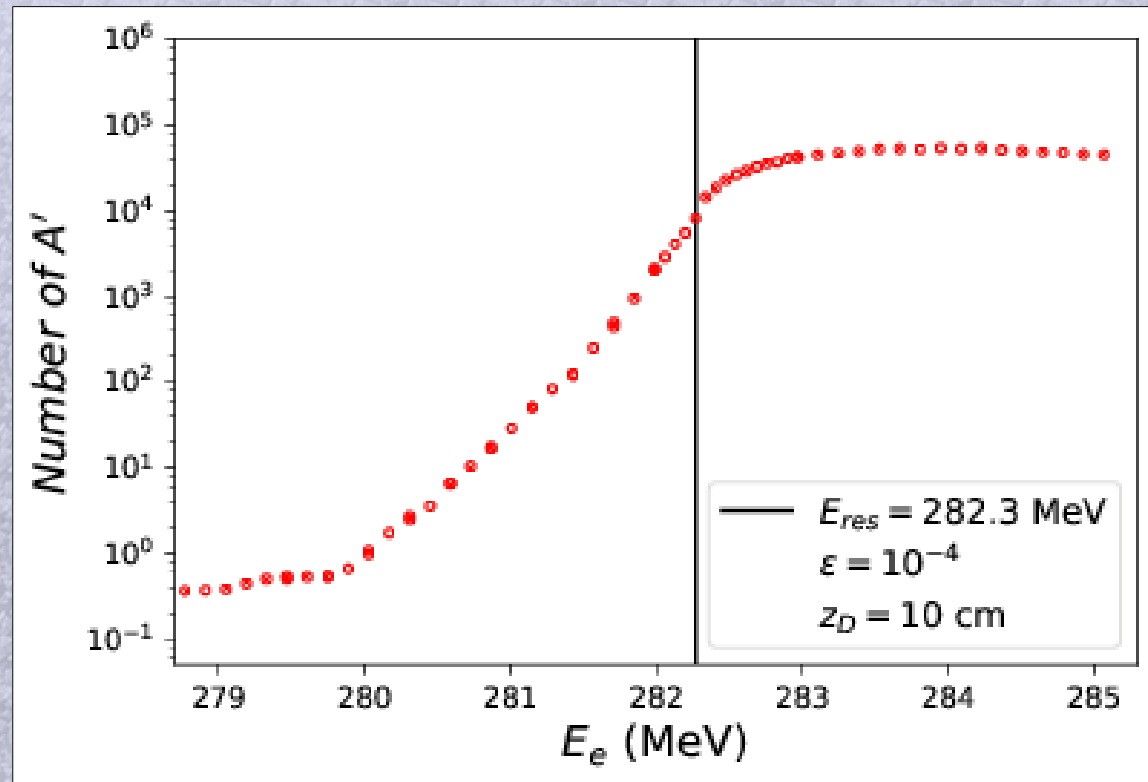
Peculiarities and advantages

**** Number of DP outside the dump**



Peculiarities and advantages

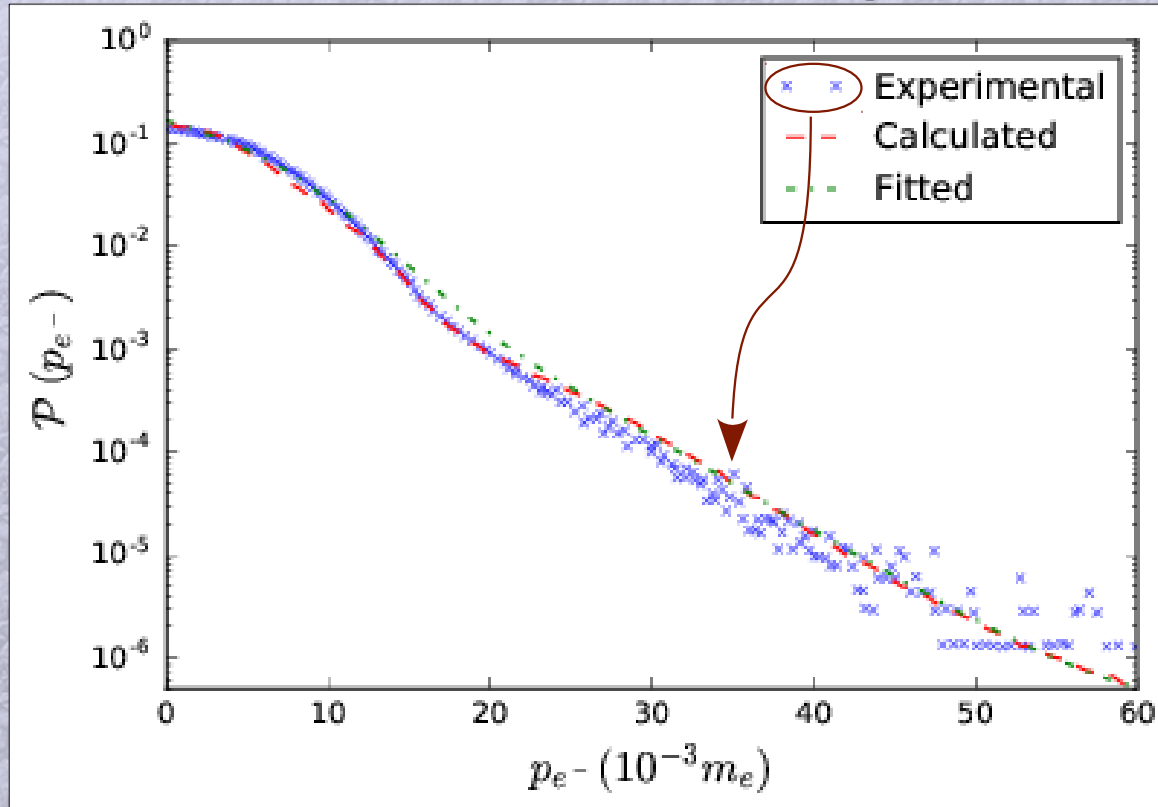
** Number of DP outside the dump



** Modifications of A' production rates from **momentum distribution of target electrons (which are not at rest)**.

Annihilation probability distribution

→ Measured in the Doppler broadening of the $e^+e^- \rightarrow \gamma\gamma$ radiation.

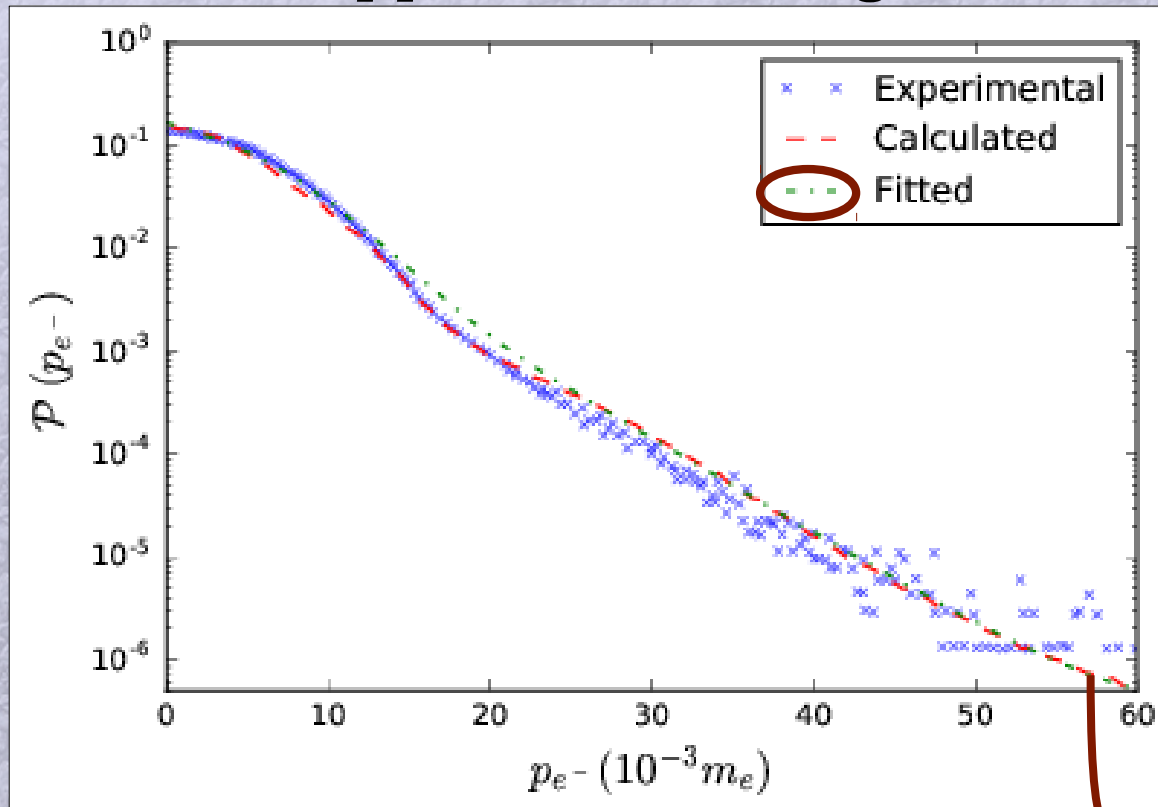


e^+ annihilation probability as a function of the target e^- momentum (for tungsten).

Figure adapted from V. J. Ghosh et al. Phys. Rev. B(2000)

Annihilation probability distribution

→ Measured in the Doppler broadening of the $e^+e^- \rightarrow \gamma\gamma$ radiation.



e^+ annihilation probability as a function of the target e^- momentum (for tungsten).

$$P(P_z) = \frac{1}{12} \left[1.015^{-p_z^2} + 1.112^{-2p_z} + 3\Theta(p_z - 50) \times 10^{1/p_z - 6} \right]$$

Effects of electrons velocities

→ To take into account the V_{e^-} , the Mandelstam variable s in the cross section is replaced by:

$$s(v_e, \chi) = 2m_e \left[E_e \left(1 - \mathcal{P}(v_e) v_e \frac{1}{2} s_\chi c_\chi \right) + m_e \right]$$

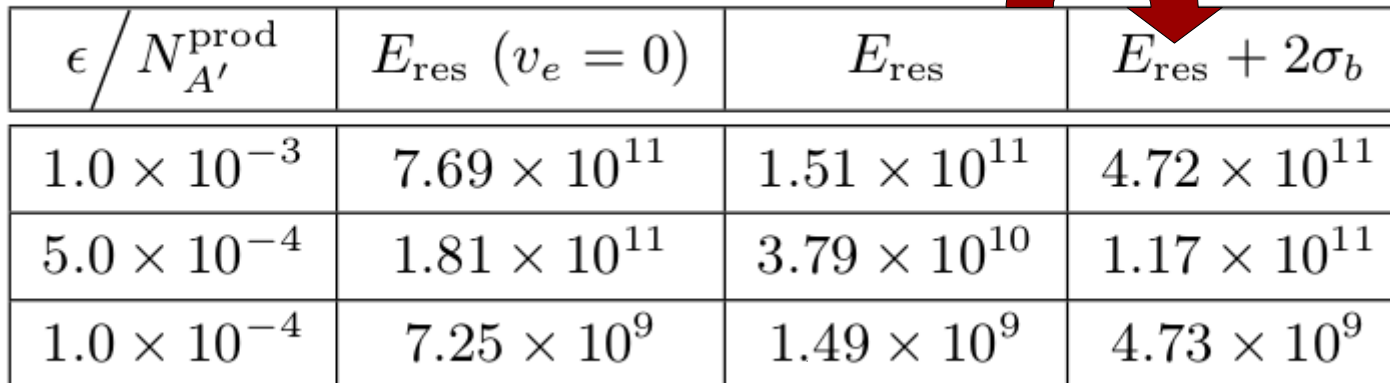
* Probability distribution for the angle X .

* Projection of V_{e^-} along the direction of the incoming e^+ .

Specific goal and Results

$\epsilon / N_{A'}^{\text{prod}}$	$E_{\text{res}} (v_e = 0)$	E_{res}	$E_{\text{res}} + 2\sigma_b$
1.0×10^{-3}	7.69×10^{11}	1.51×10^{11}	4.72×10^{11}
5.0×10^{-4}	1.81×10^{11}	3.79×10^{10}	1.17×10^{11}
1.0×10^{-4}	7.25×10^9	1.49×10^9	4.73×10^9

Specific goal and Results



$\epsilon / N_{A'}^{\text{prod}}$	$E_{\text{res}} (v_e = 0)$	E_{res}	$E_{\text{res}} + 2\sigma_b$
1.0×10^{-3}	7.69×10^{11}	1.51×10^{11}	4.72×10^{11}
5.0×10^{-4}	1.81×10^{11}	3.79×10^{10}	1.17×10^{11}
1.0×10^{-4}	7.25×10^9	1.49×10^9	4.73×10^9

Results for $m_{A'} = 17 \text{ MeV}$

→ The Atomki anomaly in ${}^8\text{Be}$ nuclear decays

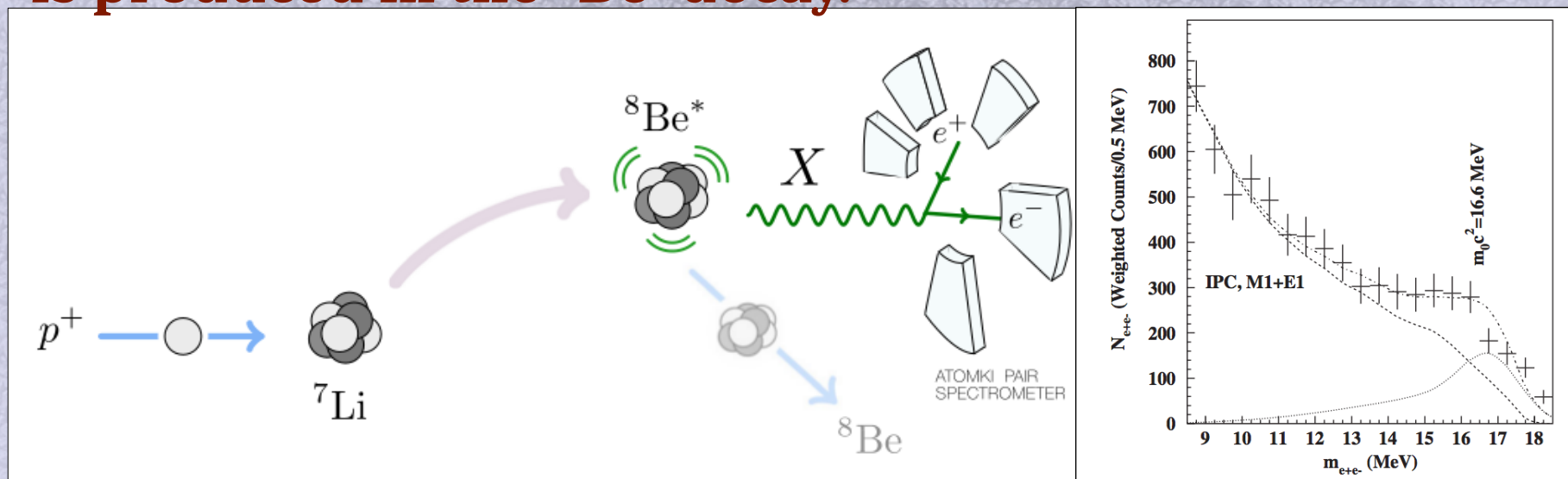
Specific goal and Results

The Atomki anomaly in ${}^8\text{Be}$ nuclear decays

A bump in the opening angle and invariant mass distributions of e^+e^- pairs produced in the decays of an excited ${}^8\text{Be}^*$ nucleus.

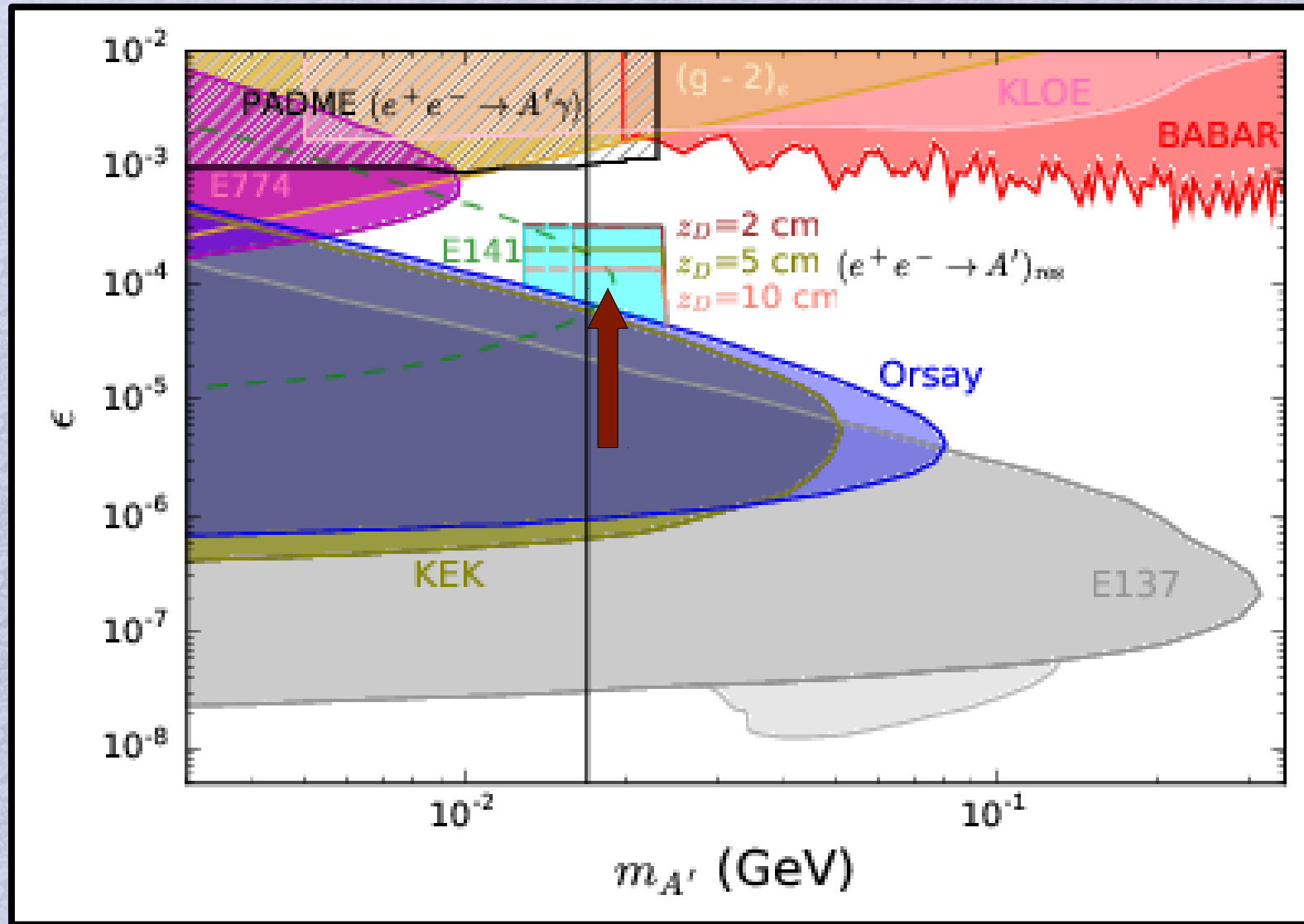
* A high statistical significance (**6.8σ**).

* The shape of the excess is consistent with that expected if a new particle with $m_{A'} = 17.0 \pm 0.2(\text{stat}) \pm 0.5(\text{sys}) \text{ MeV}$ is produced in the ${}^8\text{Be}^*$ decay.



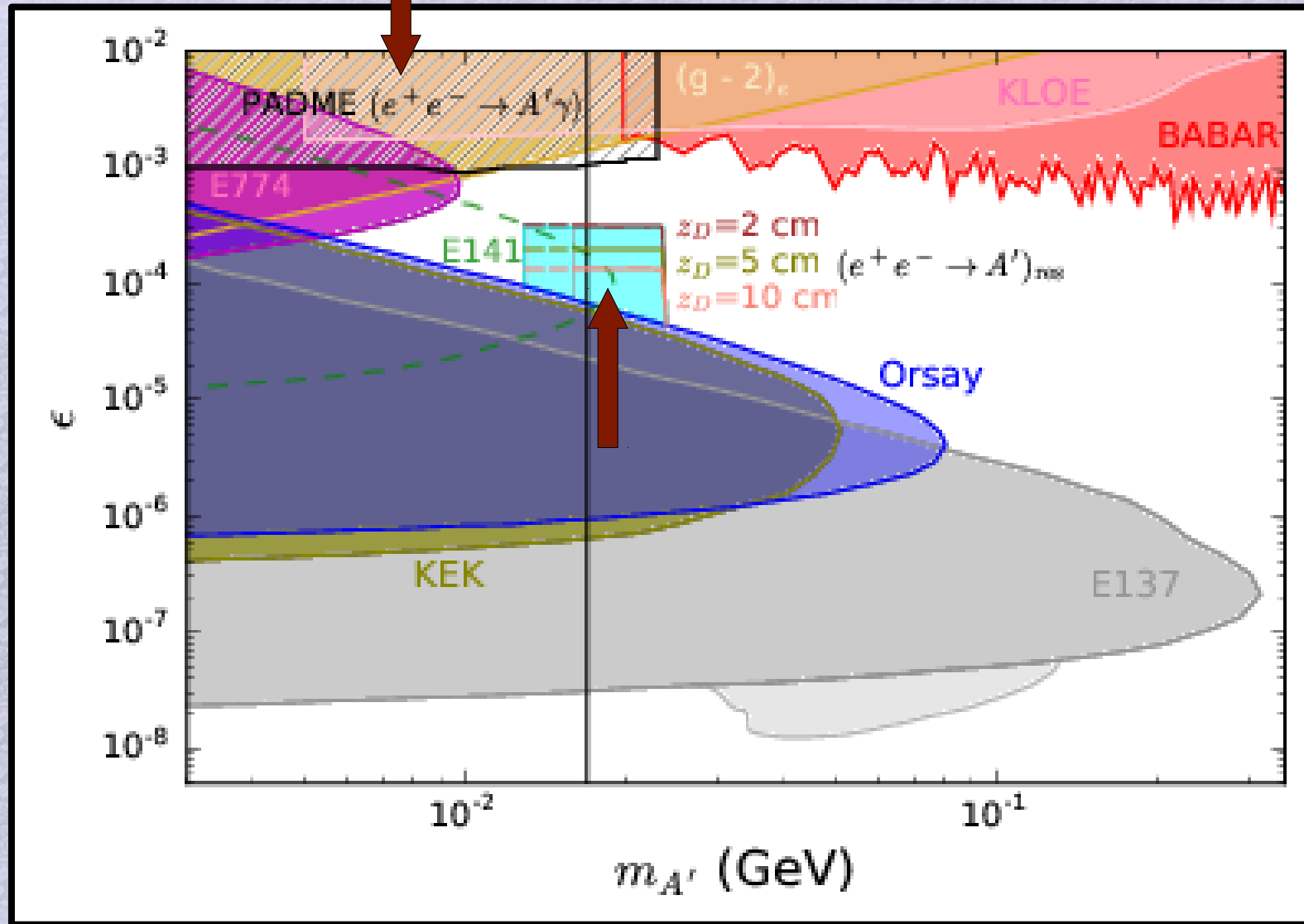
A. Krasznahorkay et al. PRL. 117, 071803, 2016 J. L. Feng et al. PRD 95, 035017, 2017

Results



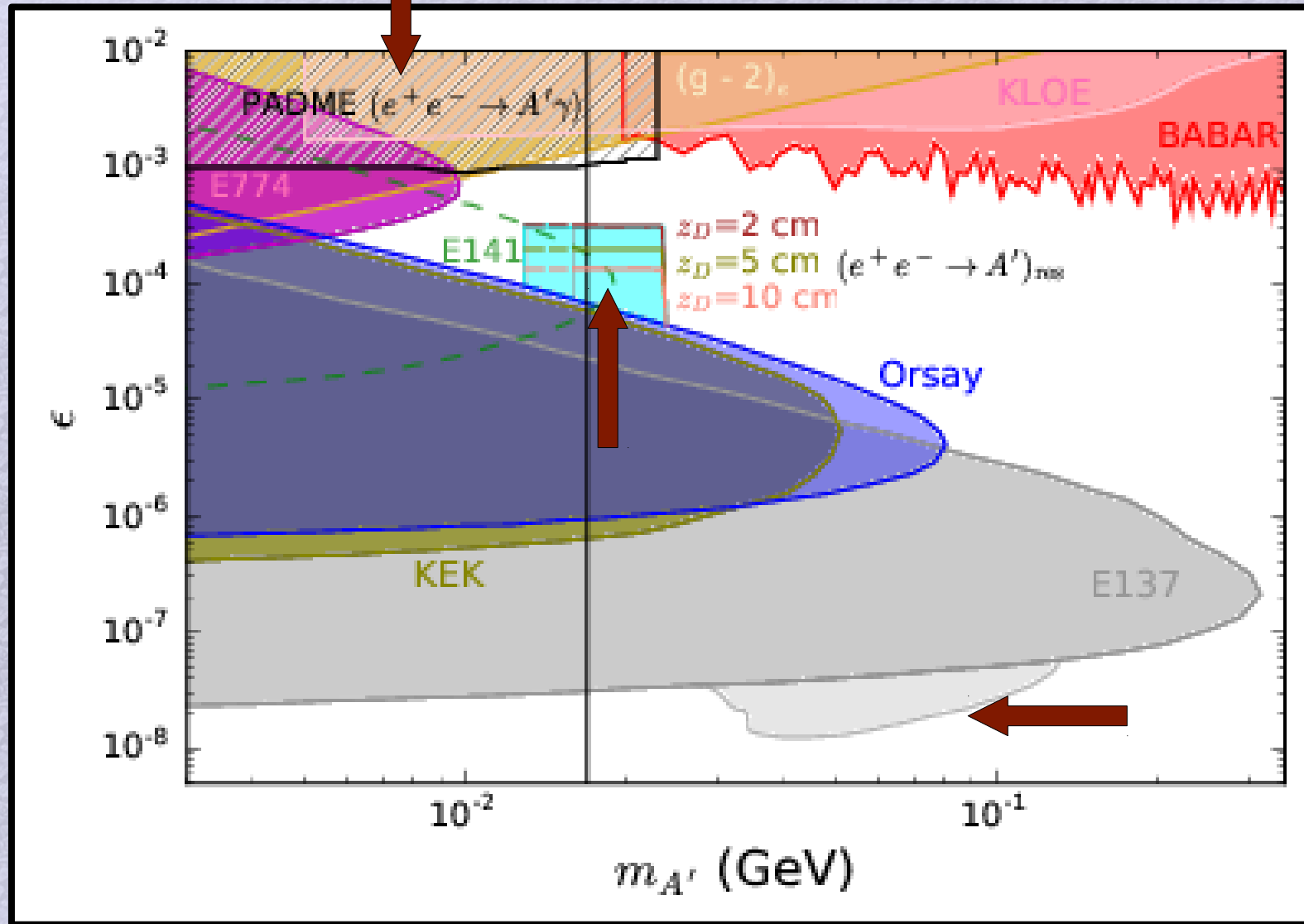
DP parameter space

Results



DP parameter space

Results

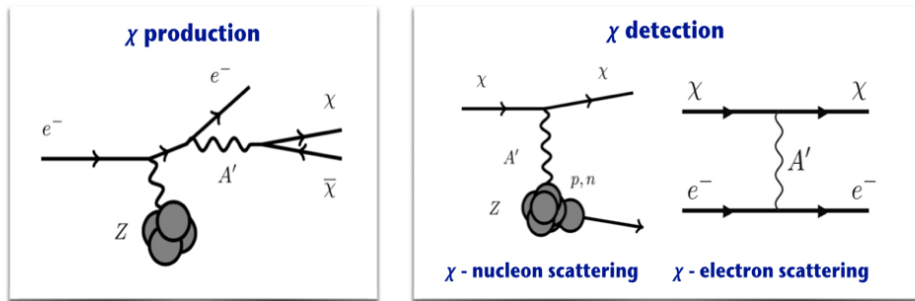
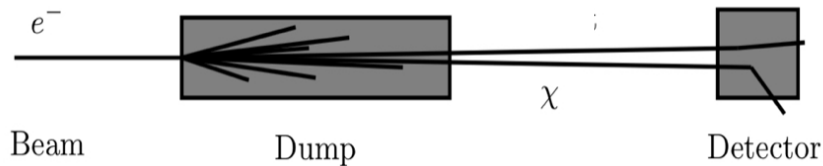


DP parameter space

L. Marsicano et al. PRD. 98, 015031 (2018)

Results

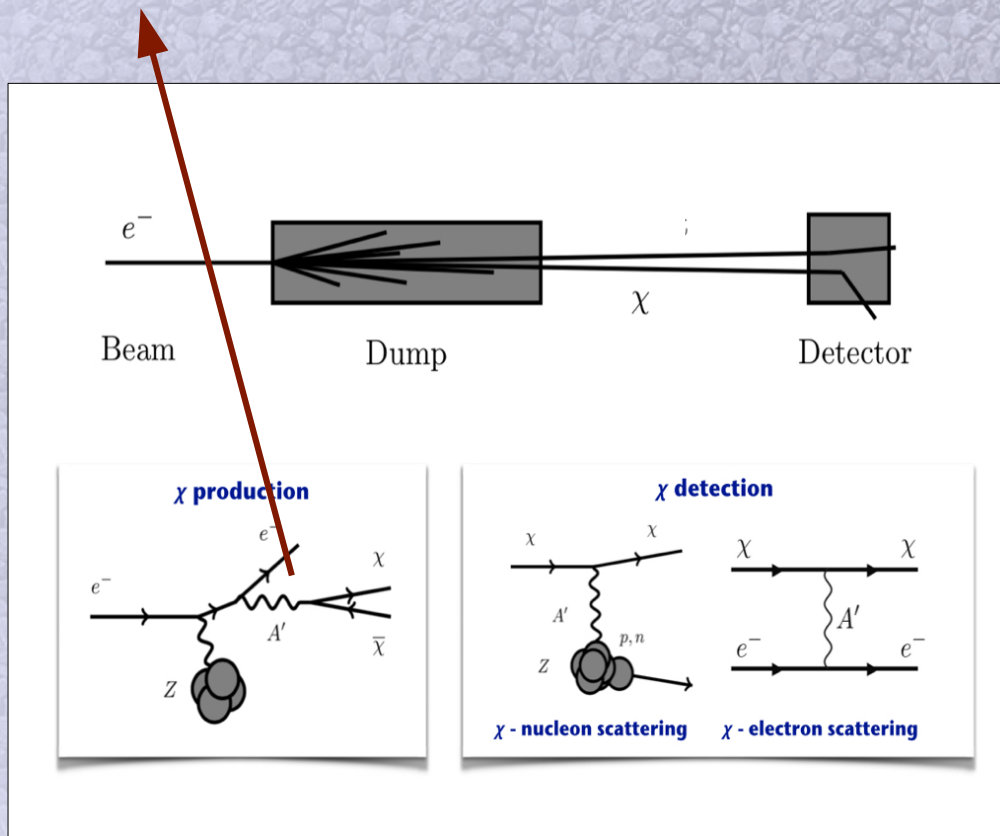
EM shower in accelerator-based experiments that make use of an intense e^- beam of moderate energy $\sim(10-20)$ GeV dumped on a thick target, **using the DP resonance (and non-resonant) production mode** (considering a subsequent decay into invisible sector) allow to produce and detect light DM $\sim(1 \text{ MeV}-1 \text{ GeV})$.



Results

EM shower allow to produce and detect light DM

SM-DM interaction
resulting in an effective
light DM secondary beam.

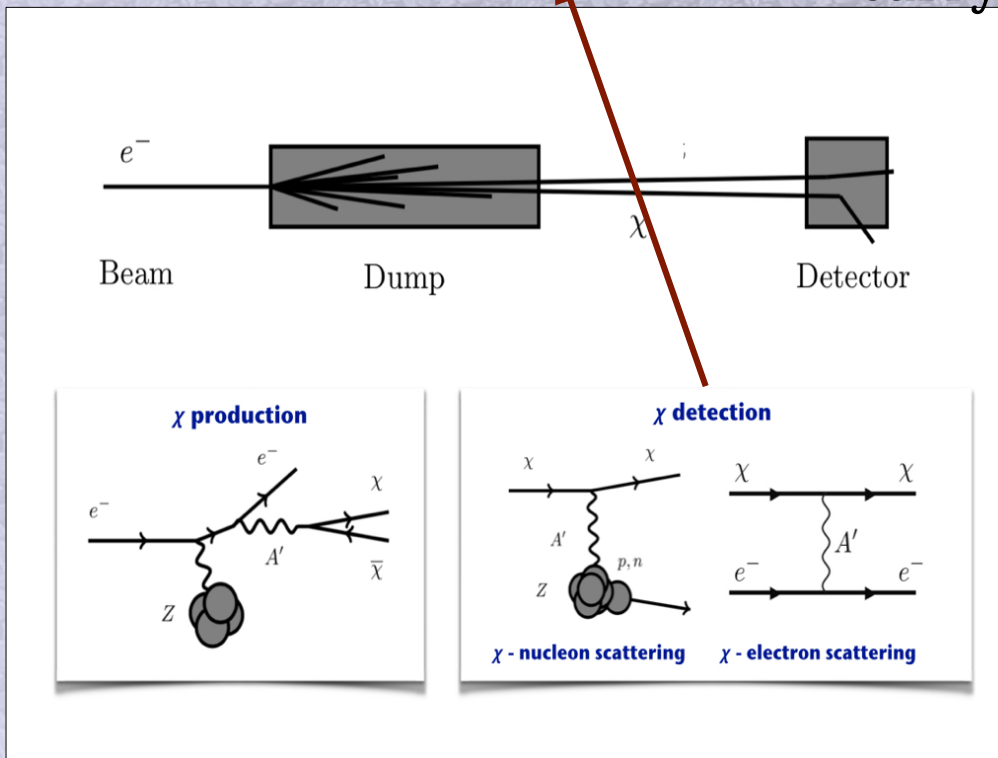


Results

EM shower allow to produce and detect light DM

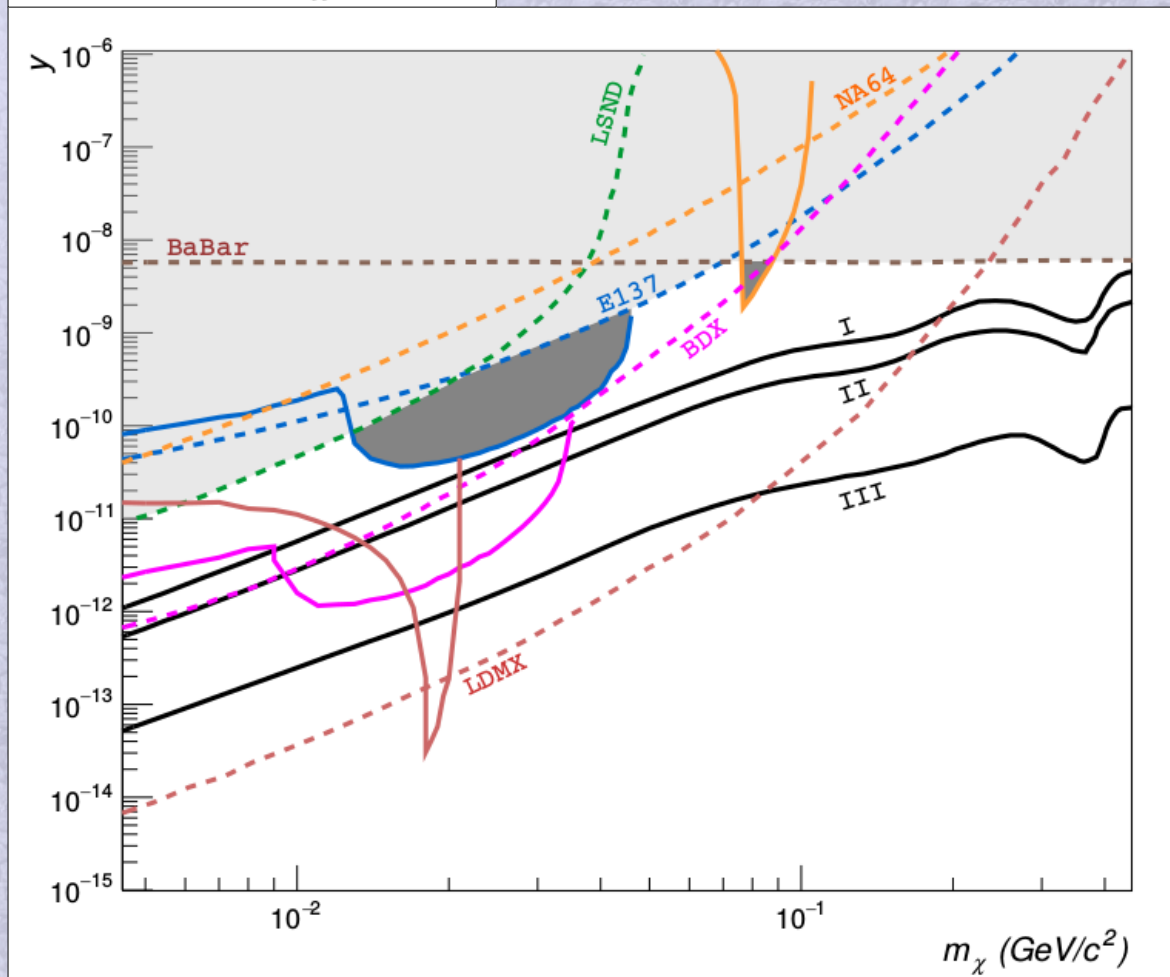
Scattering on e^- and nuclei of the detector active material may result in a detectable signal.

→ Its invisible decay products will carry away **a significant fraction of the primary beam energy**, thus resulting in a visible defect in the energy deposited in the active dump.



Results

$$y \equiv \alpha_D \epsilon^2 (m_\chi / m_{A'})^4$$

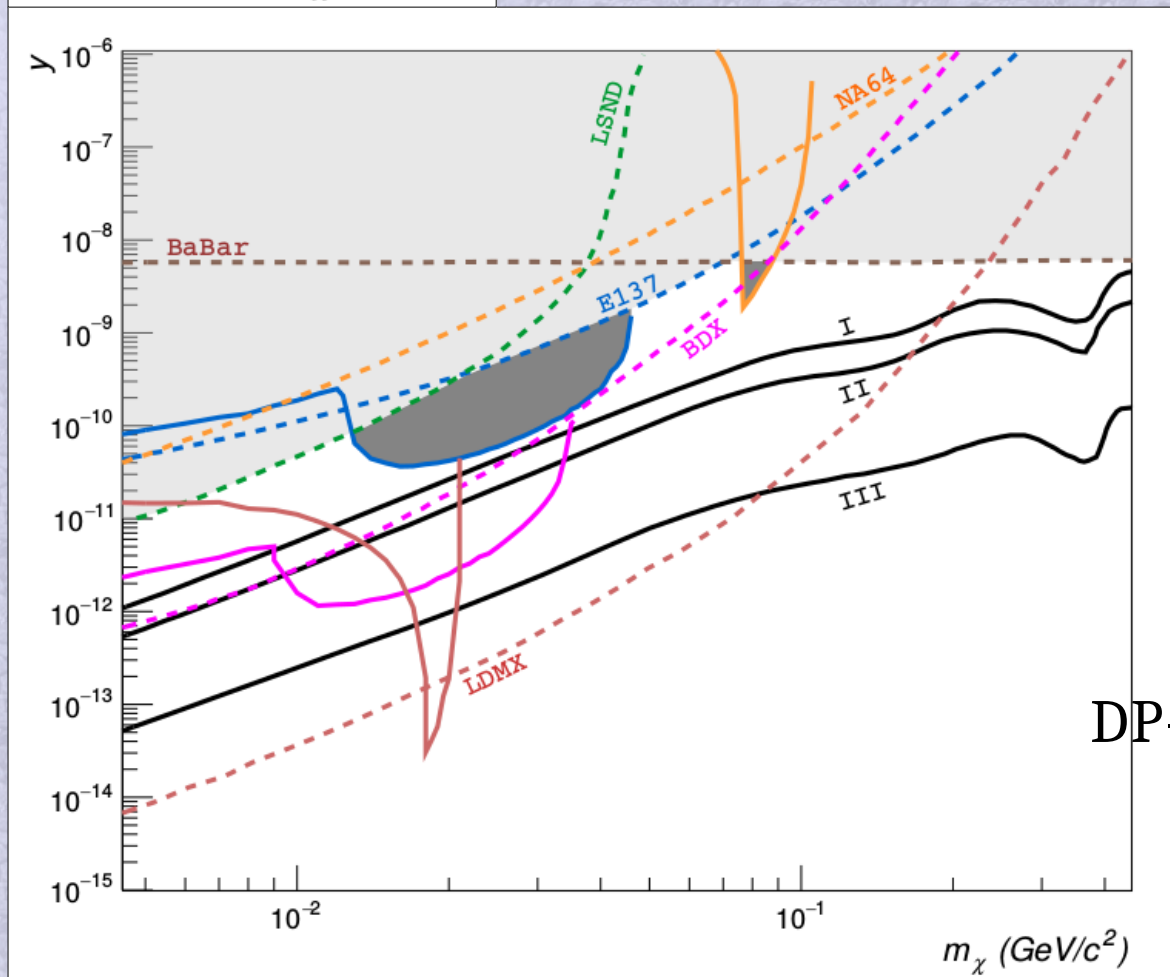


Exclusion limits at 90% C.L. obtained considering the e^+ annihilation mechanisms.

L. Marsicano et al. PRL. 121, 041802 (2018)

Results

$$y \equiv \alpha_D \epsilon^2 (m_\chi / m_{A'})^4$$



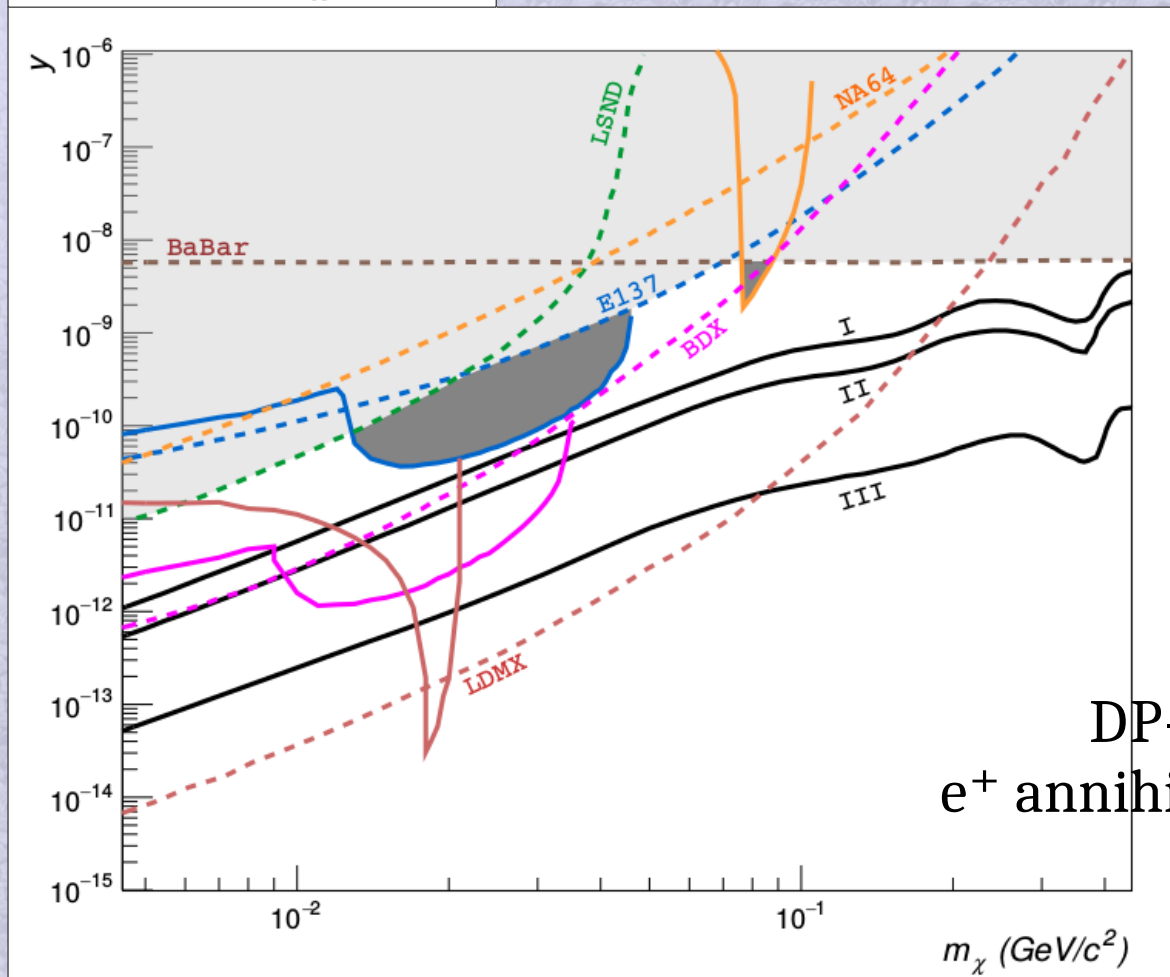
DP-strahlung (dashed lines)

Exclusion limits at 90% C.L. obtained considering the e^+ annihilation mechanisms.

L. Marsicano et al. PRL. 121, 041802 (2018)

Results

$$y \equiv \alpha_D \epsilon^2 (m_\chi / m_{A'})^4$$



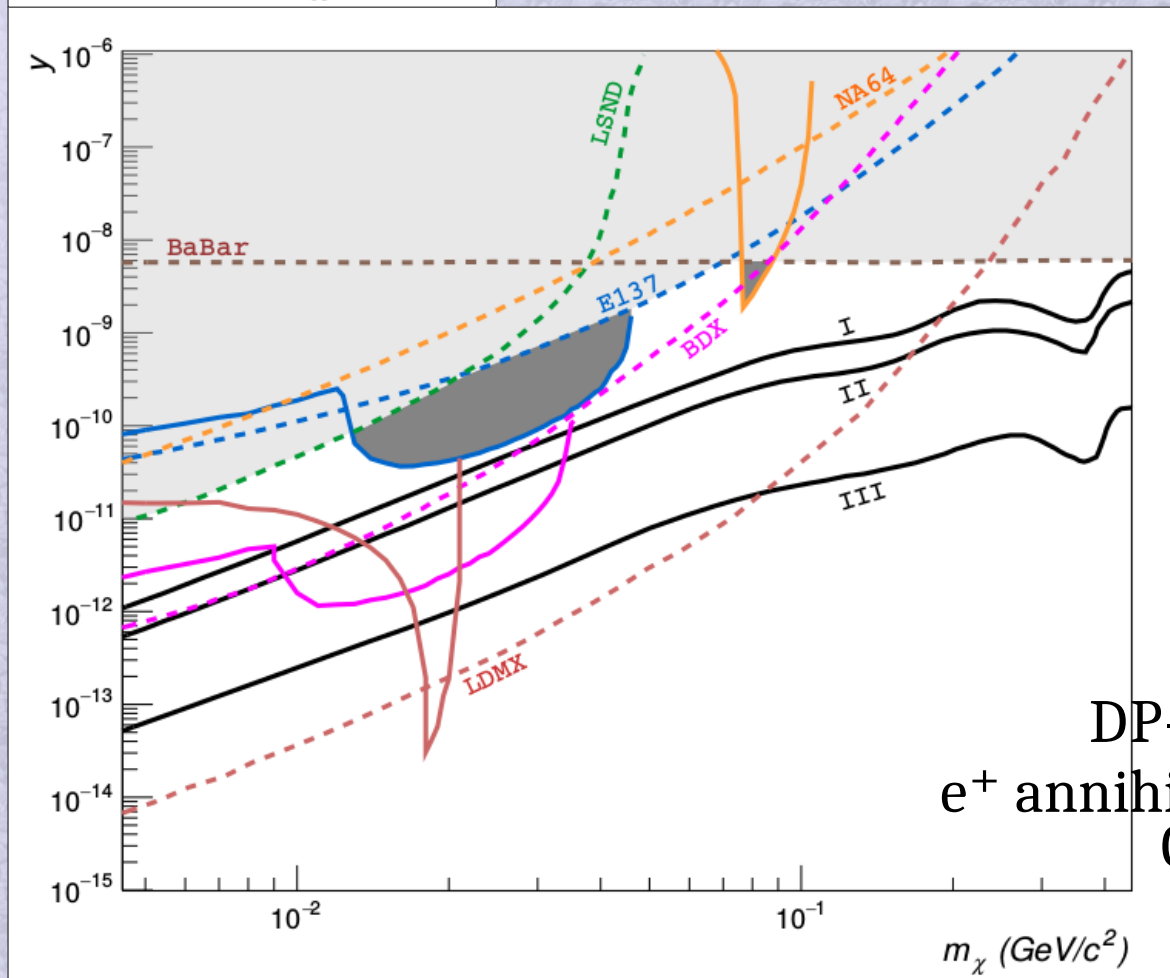
DP-strahlung (dashed lines)
 e^+ annihilation (continuous lines)

Exclusion limits at 90% C.L. obtained considering the e^+ annihilation mechanisms.

L. Marsicano et al. PRL. 121, 041802 (2018)

Results

$$y \equiv \alpha_D \epsilon^2 (m_\chi / m_{A'})^4$$



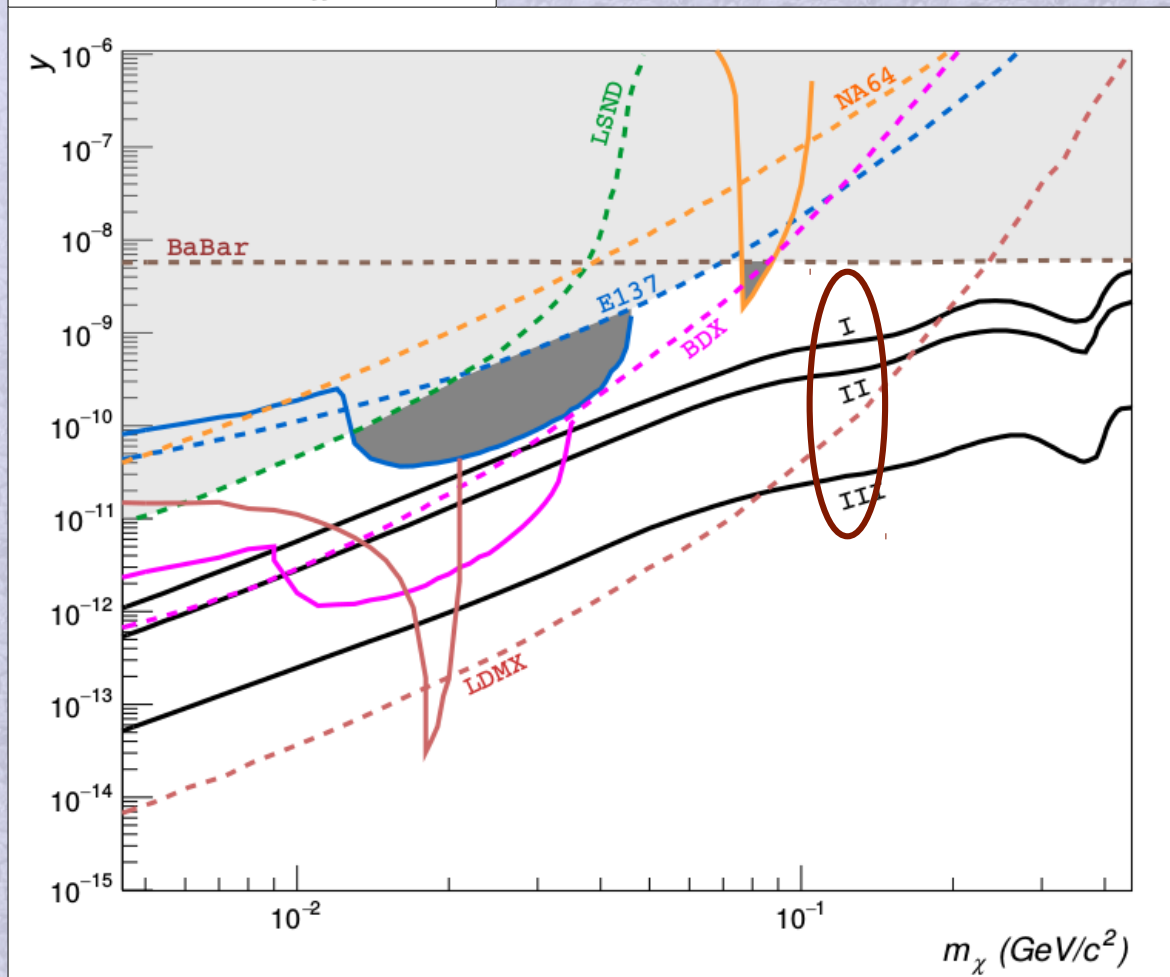
DP-strahlung (dashed lines)
e⁺ annihilation (continuous lines)
Combination (filled area)

Exclusion limits at 90% C.L. obtained considering the e⁺ annihilation mechanisms.

L. Marsicano et al. PRL. 121, 041802 (2018)

Results

$$y \equiv \alpha_D \epsilon^2 (m_\chi / m_{A'})^4$$



Thermal relic target for different hypotheses on the light DM nature:
(I) Elastic and inelastic scalar
(II) Majorana fermion
(III) Pseudo-Dirac fermion

Exclusion limits at 90% C.L. obtained considering the e^+ annihilation mechanisms.

L. Marsicano et al. PRL. 121, 041802 (2018)

Conclusions

A new way to search DP, coupled to e^+e^- pairs, via resonant production in e^+e^- annihilation is suggested as an alternative method to test new physics at high-intensity accelerators.

With this alternative is possible cover the center of mass energy needed to produce, via resonant e^+e^- annihilation, the $m_{A'} = 17$ MeV DP invoked to explain the anomaly ^8Be .

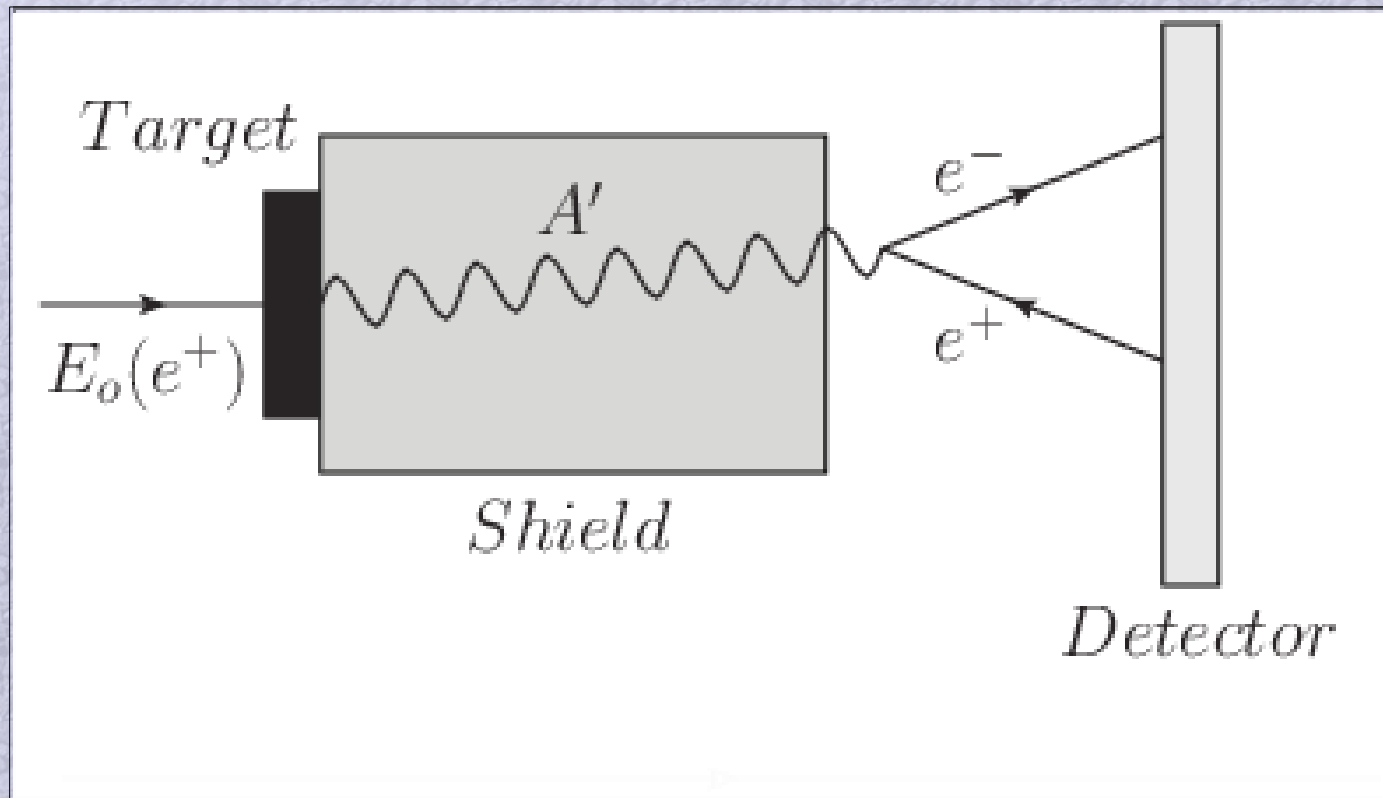
Resonant e^+e^- annihilation needs to be included for a correct evaluation of exclusion limits obtained from electron beam-dump experiments.

Thank you !



XII Latin America Symposium on High Energy Physics

Sketch of a positron beam dump experiment



Comparing A' production modes

Production mode	E_{beam} (MeV)	T [integration]	A' produced
Bremsstrahlung (e^-)	550	0.5	4.1×10^7
Annihilation (e^+)	550	0.5	8.7×10^8
Resonant (e^+)	$E_{\text{res}} = 282 \text{ MeV}$	[0 - 0.5]	7.2×10^9
Resonant (e^+)	$E_{\text{res}} + 2\sigma_{\text{beam}}$	[0 - 0.5]	12.2×10^9

Momentum distribution of electrons in tungsten

Electron shell	n_{nl}	Z_{eff} [21]	$\langle v_{nl} \rangle$
1s	2	72.57	0.53
2s	2	54.67	0.40
2p	6	69.57	0.51
3s	2	51.87	0.38
3p	6	52.62	0.38
4s	2	40.56	0.30
3d	10	60.45	0.44
4p	6	39.55	0.29
5s	2	23.54	0.17
4d	10	37.17	0.27
5p	6	21.33	0.16
6s	2	9.85	0.07
4f	14	34.71	0.25
5d	4	16.74	0.12

Table I. Tungsten electron structure, effective nuclear charge Z_{eff} (taken from [21]) and average electron velocity for each electron subshell. In the second column n_{nl} is the number of electrons in each subshell.

The average velocities for each subshell are estimated via the virial theorem.

This gives an indication of the relevance of including the target electrons momentum.

Electron shell	n_{ln}	Z_{eff} [21]	$\langle v_{nl} \rangle$
1s	2	5.67	0.04
2s	2	3.22	0.02
2p	2	3.14	0.02

Table II. Carbonium electron structure, effective nuclear charges Z_{eff} [21] and average electron velocity for each electron subshell. In the second column n_{nl} is the number of electrons in each subshell.

Comparing with carbon